The electronic structure of a weakly correlated antiferromagnetic metal, $SrCrO_3$: first-principles calculations

2011 New J. Phys. 13 053002

(http://iopscience.iop.org/1367-2630/13/5/053002)

New Journal of Physics
The open-access journal for physics

The electronic structure of a weakly correlated antiferromagnetic metal, $SrCrO_3$: first-principles calculations

Yumin Qian[1,3], Guangtao Wang[2], Zhi Li[1], C Q Jin[1] and Zhong Fang[1]

[1] Beijing National Laboratory for Condensed Matter Physics and Institute of Physics, Chinese Academy of Sciences, Beijing 100190, China
[2] Department of Physics, Henan Normal University, Xinxiang 453007, China
E-mail: yuminqian@gmail.com

New Journal of Physics **13** (2011) 053002 (16pp)
Received 10 December 2010
Published 3 May 2011
Online at http://www.njp.org/
doi:10.1088/1367-2630/13/5/053002

Abstract. On the basis of our idea of degree modulation, by using systematic first-principles calculations, we study the electronic structure and magnetic properties of $SrCrO_3$. Our results suggest that $SrCrO_3$ is a weakly correlated antiferromagnetic (AF) metal, a very rare situation in transition-metal oxides. Among various possible AF states, C-type spin ordering with a small amount of orbital polarization (the d_{xy} orbital is more occupied than the $d_{yz/zx}$ orbital) is favored. The detailed understanding of the mechanism that stabilizes the C-type AF state is analyzed on the basis of the competition between itinerant Stoner instability and superexchange, and our results suggest that magnetic instability rather than lattice or charge instabilities plays an important role in this system. The experimentally observed *c*-axis compressed tetragonal distortion can be naturally explained with the C-type AF state. By using the LDA + U method to study this system, we show that the wrong ground state will be obtained if U is large.

[3] Author to whom any correspondence should be addressed.

Contents

1. Introduction

The electronic and magnetic structures of transition metal compounds with a partially filled d shell are usually complicated, owing to the mutual interplay of various degrees of freedom [1]–[4], such as lattice, spin, charge and orbital. The relative competition or cooperation among these degrees of freedom may stabilize many possible states, which are energetically close. It is a challenging issue to identify these subtle energy differences between various possible solutions. Nevertheless, first-principles electronic structure calculations based on density functional theory provide the possibility of elucidating the detailed difference between these solutions and uncovering the mechanisms that govern their properties if we could systematically study the impact of these degrees of freedom on its electronic structure. To achieve this goal, we introduce the concept of degree modulation, which first freezes all degrees of freedom and then activates them one by one, to see the evolution of the physical trend. Such a strategy will be followed in this paper to study the electronic and magnetic properties of $SrCrO_3$, a simple perovskite but having many controversial issues [5]–[8].

Limited knowledge is available about $SrCrO_3$, owing to the necessity of high pressure for synthesis [5]. Chamberland [6] first reported $SrCrO_3$ as a Pauli paramagnetic metal with cubic perovskite structure; however, in a recent study by Zhou *et al* [5], it is suggested to be a cubic paramagnetic insulator with possible insulator-to-metal transition under a pressure of 4 GPa in their polycrystal samples. Several anomalous properties, such as deviating the Curie–Weiss law of magnetic susceptibility, low Seebeck coefficient, and glassy thermal conductivity, are reported in Zhou *et al*'s study, and those properties are attributed to the bond-length fluctuation instabilities. On the other hand, a new structural phase, i.e. perovskite with compressive tetragonal distortion, was reported recently for $SrCrO_3$ by Attfield and co-workers [7]. A cubic-to-tetragonal structure transition was observed around 40 K; however, no discontinuity in electronic conductivity was observed owing to the coexistence of both the cubic and the tetragonal phases, even at low temperature. The relative instability of the two structural phases is sensitive to sample preparation and microstrain. Attfield and co-workers [7] also suggested that in the tetragonal phase, the C-type AF state with partial orbital ordering is favored. Alario-Franco *et al* [8] again reported $SrCrO_3$ as a cubic paramagnetic metal, and suggested the 4 + oxidation state of Cr (i.e. Cr^{4+}) by electron energy loss spectroscopy (EELS). No anomaly was found in their specific heat measurement for $SrCrO_3$ [9].

On the theoretical side, Lee and Pickett [10] studied the electronic structure of $SrCrO_3$ by using first-principles calculations. Their results suggested that C-type AF spin ordering is the most stable ground state, and the orbital ordering leads to the tetragonal lattice distortion. They also found a strong magneto-phonon coupling for the oxygen octahedral breathing mode and an orbital ordering transition by LDA + U calculation. Streltsov *et al*'s [11] and Komarek *et al*'s [12] work focuses on $CaCrO_3$, an isovalent compound with orthorhombic $GdFeO_3$-type distortion. Their results suggested that $CaCrO_3$ is an intermediate-correlated metal with a similar C-type AF ground state, and $SrCrO_3$ is more itinerant than $CaCrO_3$, making this system especially interesting from both the experimental and the theoretical points of view.

In summary, the electronic conductivity, lattice structure, magnetic properties and origin of orbital ordering are still unclear. Furthermore, $SrCrO_3$, together with a few other antiferromagnetic (AF) metallic examples, such as $CaCrO_3$ [11], $(La/Sr)_3Mn_2O_7$ [13] and $Ca_3Ru_2O_7$ [14], provides exceptions to the general relation between magnetic order and electrical conductivity [15]: ferromagnetism typically coexists with metallic conductivity, whereas insulators usually exhibit antiferromagnetism. It is also challenging and interesting to try to understand these exceptions; a clear understanding of the basic electronic structure of $SrCrO_3$ will help us to better understand the relationship between spin–orbital ordering and conductivity.

In order to clarify the above issues and understand the mechanism of the ground state of $SrCrO_3$, in this work we perform first-principles calculations for this compound. From the calculated results, controversial issues regarding its conductivity (metal or insulator) and lattice structure (cubic or tetragonal) can be naturally clarified based on our systematic analysis. We conclude that the *c*-axis compressed tetragonal structure with C-type AF spin ordering is the most stable state. A mechanism is proposed for understanding the stabilization of such a C-type AF metallic state. In contrast to earlier studies [5, 10], we suggest that magnetic instability rather than lattice or charge instabilities plays an important role in this system. This paper is organized as follows. The methods will be described in section 2, and the results and discussions, which are separated into four subsections step by step, will be presented in section 3. Finally, a brief summary will be given in section 4.

2. The method

First-principles calculations based on the density functional theory were performed by using the BSTATE (Beijing Simulation Tool for Atom Technology) package [16], in which the plane-wave pseudopotential method [17] is adopted. The 3d states of Cr and 2p states of O are treated with the ultrasoft pseudopotential [18] and other states are treated with the optimized norm-conserving pseudopotential [19]. The cut-off energy for describing the wave functions is 36 Ry, while that for the augmentation charge is 200 Ry. We use an $(8 \times 8 \times 8)$ mesh for *k*-points sampling in the linear tetrahedron method with curvature correction. For the exchange-correlation energy, local density approximation (LDA) is used. We further use the LDA + *U* method to study the effect of electron correlation [16]. Virtual crystal approximation (VCA) [20] is used to study the effect of doping.

Both the cubic and the tetragonal perovskite structures with full lattice relaxation are studied. For each fixed crystal structure, various different magnetic states are studied. They are the non-magnetic (NM) state, the ferromagnetic (FM) state, the layered-type antiferromagnetic (A-type AF) state, the chain-type antiferromagnetic (C-type AF) state and the conventional

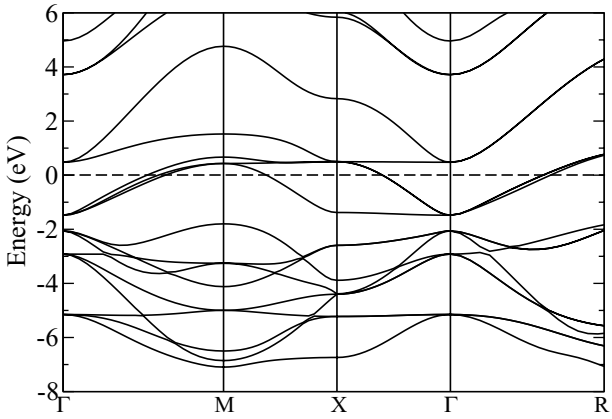

Figure 1. Band structure of NM $SrCrO_3$ in the cubic structure along high-symmetry lines. The Fermi level E_F is at 0.0 eV.

antiferromagnetic (G-type AF) state [1]. Local atomic orbitals of the Cr atom are defined to calculate the orbital occupation and its ordering.

3. Results and discussions

In order to clearly understand the physics, in this study, we use the following strategy of degree modulation: it is better to separate the contributions coming from different degrees of freedom, such as spin, orbital, lattice and charge. Starting from the simplest situation where various degrees of freedom are frozen (not involved), we add the effects of different degrees of freedom one by one to observe the evolution of the electronic structure; finally, the effects of various degrees of freedom, the interplay among these degrees of freedom and the possible correlation effects are carefully studied step by step.

3.1. Basic electronic structure of non-magnetic (NM) $SrCrO_3$ in the cubic structure

An excellent previous work by Lee *et al* [10] gives a good description in the NM case. Although our work is closely similar to theirs, it is still necessary to present here our study to motivate further in-depth studies of this compound and to make our strategy complete.

The nominal atomic valences in $SrCrO_3$ are Sr^{2+}, Cr^{4+} and O^{2-}, respectively, where the 2p states of O^{2-} are fully occupied, and the 3d shell of Cr^{4+} is filled with two electrons, similar to d^2 systems such as $LaVO_3$ and YVO_3 [21, 22] and CrO_2 [23]. Since the atomic levels of Sr^{2+} are far away from the Fermi level, the electronic properties of $SrCrO_3$ are mostly determined by the p–d bonding between Cr-3d and O-2p. Figures 1 and 2 show the electronic band structure and DOS of NM $SrCrO_3$ in the cubic perovskite structure, calculated with an experimental lattice parameter (space group $Pm3m$, $a = 3.811$ Å) [7]. The states from -7.4 to -1.6 eV are mostly from the O-2p bonding orbitals, and the states around the Fermi level E_f (from -1.5 eV to 5.0 eV) are from Cr-3d antibonding orbitals, as shown by the PDOS in figure 2. The p–d hybridization is substantial, and the total DOS at the Fermi level is about 1.48 (states per eV spin f.u.).

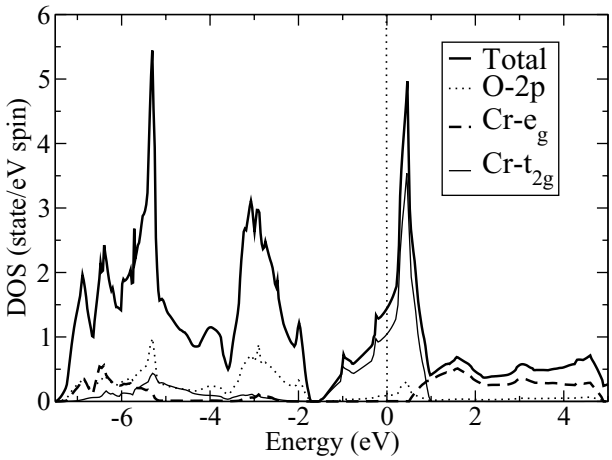

Figure 2. The density of states (DOS) and projected DOS (PDOS) of NM $SrCrO_3$ in the cubic perovskite structure. The Fermi level is at zero energy. The sharp DOS peak around 0.5 eV is due to the flat band segments visible in figure 1.

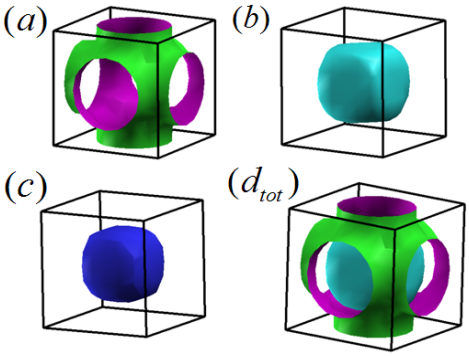

Figure 3. The Fermi surfaces (FS) of NM cubic $SrCrO_3$. (a–c) The three sheets of FS and (d_{tot}) the display for total three sheets. The Γ-point is located at the center of the cube.

Due to the octahedral local crystal field, the five d orbitals of Cr split into a lower-lying threefold degenerate t_{2g} manifold and a higher twofold degenerate e_g manifold. The bandwidth of the t_{2g} and e_g states is about 2.5 and 4.2 eV, respectively. The bandwidth of e_g is much larger than that of t_{2g}, because $pd\sigma$-type bonding is stronger than $pd\pi$-type bonding. The t_{2g}–e_g separation (crystal field splitting) is about 2.4 eV, comparable to the t_{2g} bandwidth. The Fermi level E_f lies within the t_{2g} manifold, whereas the e_g part lies well above E_f, suggesting a typical t_{2g} system. The calculated total occupation number of Cr-3d orbitals is $n = 1.994$, quite consistent with chemical stoichiometry analysis and the EELS experiment, which suggests the Cr^{4+} valence state of Alario-Franco [9].

All three t_{2g} bands cross the Fermi level, forming three sheets of FS, as shown in figure 3. There is also a large section of flat band structure along $\Gamma(0, 0, 0) - X(0, \pi, 0) - M(\pi, \pi, 0)$ high-symmetry lines, which leads to the sharp DOS peak located 0.5 eV above E_f. The existence of such Van-Hove singularity will affect the electronic structures considerably, as will be addressed below. Among the three sheets of FS, two of them are cubic-like with flat facets,

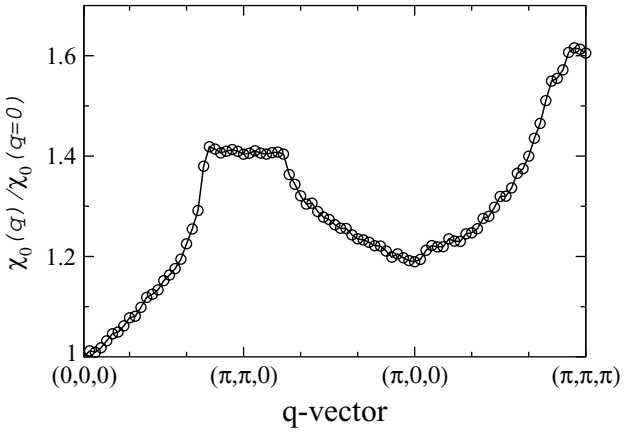

Figure 4. The calculated Lindhard response function $\chi_0(q)$ for q vectors along the high-symmetry lines Γ–M–X–R of NM cubic $SrCrO_3$. There are two structures around $q = (\pi, \pi, 0)$ and $q = (\pi, \pi, \pi)$, respectively, corresponding to two different kinds of possible instabilities.

suggesting the possible existence of FS nesting. The above calculation is consistent with previous work by Lee *et al* [10], who have also pointed out that FS nesting may lead to magnetic or charge instability, whereas Zhou *et al* [5] proposed lattice instability (bond-length fluctuation) in this system. So it is very interesting to clarify this controversy and identify the nature of the instability in $SrCrO_3$. To further clarify this point, we calculated the Lindhard response function $\chi_0(q)$, as shown in figure 4. There is a plateau located around $q = (\pi, \pi, 0)$ and a sharp peak located at $q = (\pi, \pi, \pi)$, with the latter peak slightly higher than the former. The presence of two structures in the response function corresponds to two kinds of magnetic instabilities, which are related to C-type and G-type AF ordering, respectively, as will be discussed in detail below. Considering the fact that the peak at $q = (\pi, \pi, \pi)$ is higher than that at $q = (\pi, \pi, 0)$, it may be expected that the G-type AF state is easier to stabilize than the C-type AF state. Unfortunately, this expectation is not consistent with our following calculations.

3.2. Magnetic instability in the cubic structure

Now we include the spin degree of freedom in our studies. For this purpose, we neglect a possible lattice distortion and concentrate only on the cubic structure. We calculate the total energies of different magnetic states as a function of volume. As shown in figure 5, the C-type AF state is always stabilized for all of the calculated volumes. In other words, the C-type AF state is the most stable state, even without any lattice distortion. This is one of our main conclusions and will be discussed in detail in this section.

From the energetic point of view, as shown in figure 5, the energy difference between the NM and FM states is small (about 54 meV f.u.$^{-1}$ if the experimental lattice parameter is used), and the FM state is easily suppressed by volume compression. On the other hand, there exists a big energy difference (more than 100 meV f.u.$^{-1}$) between the FM and various AF states, and the energy difference between various AF states (A-type, C-type and G-type) is small (about 20–50 meV f.u.$^{-1}$). In view of this fact as well as the fact, suggested by the calculated response function in figure 4, that an itinerant picture alone cannot fully explain the magnetic property,

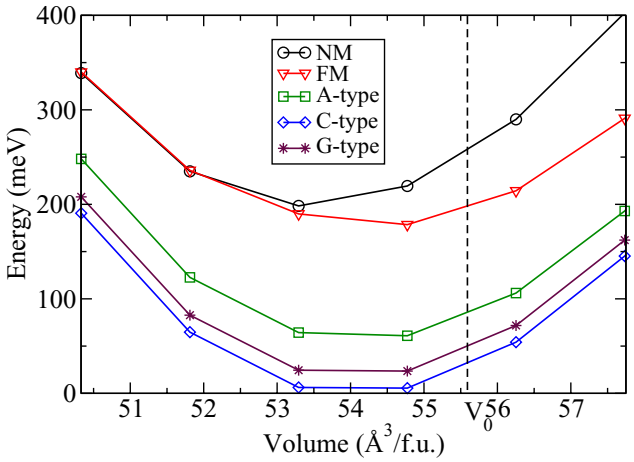

Figure 5. Calculated total energy versus volume for cubic $SrCrO_3$ in various spin states. V_0 is the experimental volume.

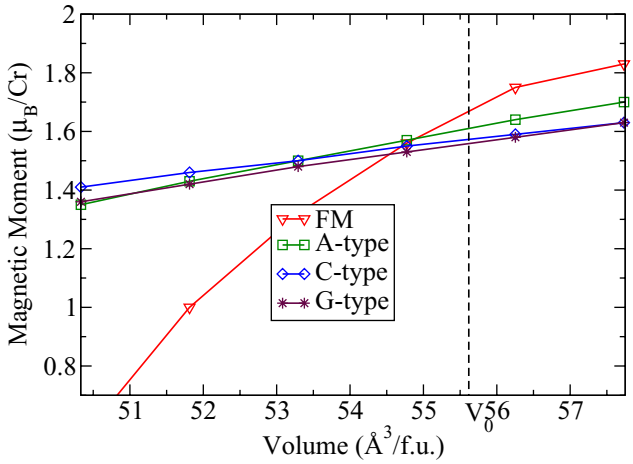

Figure 6. Calculated volume dependence of the magnetic moment for various spin states of cubic $SrCrO_3$. V_0 is the experimental volume.

the superexchange may play some role in stabilizing the AF states. The subtle balance between the itinerant kinetic energy and superexchange leads to the C-type AF ground state.

The calculated magnetic moments of various states as a function of volume are shown in figure 6. At the equilibrium volume, the high-spin states are always favored, and the magnetic moments of various states are close to $2.0\mu_B\,Cr^{-1}$, suggesting the sizable Hund's coupling. The calculated moments are $1.63\mu_B\,Cr^{-1}$, $1.59\mu_B\,Cr^{-1}$, $1.56\mu_B\,Cr^{-1}$, $1.55\mu_B\,Cr^{-1}$ for FM, A-type, C-type and G-type states, respectively. For the FM state, the magnetic moment quickly collapses with volume compression, as shown in figure 6, whereas for the AF states (A-type, C-type and G-type), the moments are not so sensitive to volume change. This again suggests that although the system is close to itinerant Stoner instability, the stabilization of AF states is beyond the Stoner mechanism.

Although we treat only the cubic structure, A-type and C-type magnetic ordering will further break the symmetry and lead to orbital ordering. As shown in figures 7–10 and listed

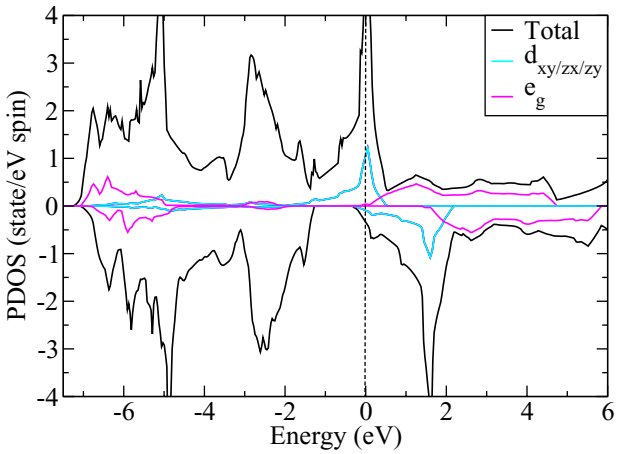

Figure 7. PDOS of the FM spin state in the cubic structure.

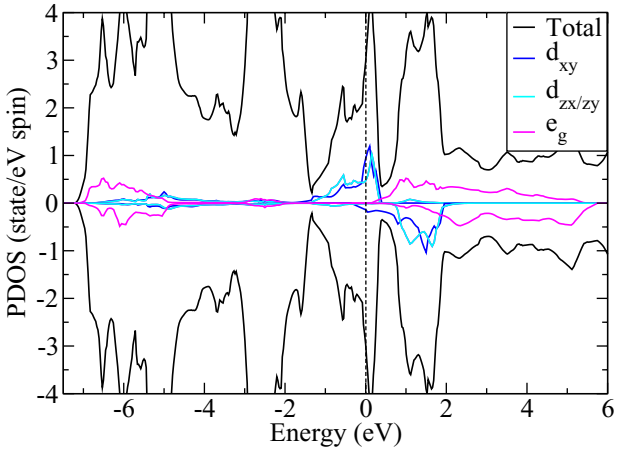

Figure 8. PDOS of the A-type AF state in the cubic structure.

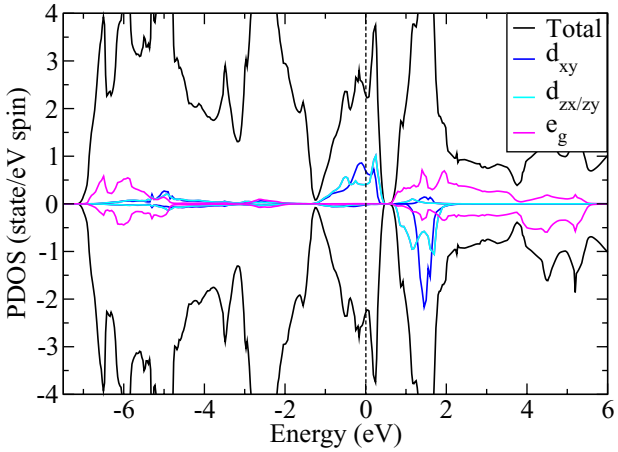

Figure 9. PDOS of the C-type AF state in the cubic structure.

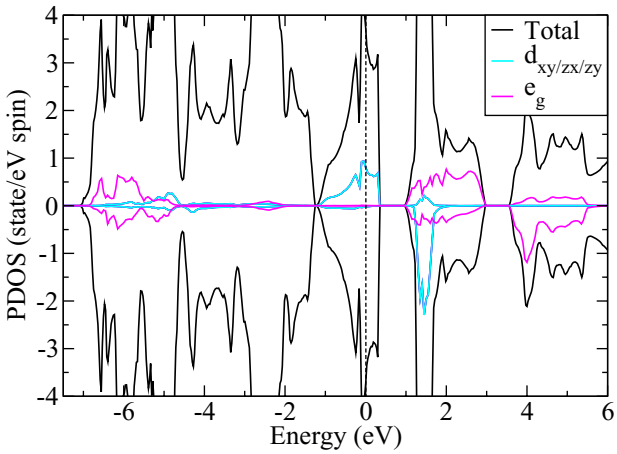

Figure 10. PDOS of the G-type AF state in the cubic structure.

Table 1. Orbital polarization, evaluated as the occupation number difference between the d_{xy} and $d_{yz/zx}$ orbitals (i.e. $n_p = n_{d_{xy}} - n_{d_{yz/zx}}$), for various magnetic states with different lattice distortions (c/a ratio).

	c/a ratio						
	1.015	1.010	1.005	1.000	0.995	0.990	0.985
FM	−0.041	−0.028	−0.014	0.000	0.015	0.028	0.042
A-type	−0.061	−0.053	−0.046	−0.038	−0.031	−0.023	−0.011
C-type	0.022	0.033	0.043	0.056	0.067	0.076	0.087
G-type	−0.031	−0.019	−0.009	0.000	0.011	0.021	0.032

in table 1, the degeneracy between the d_{xy} and $d_{yz/zx}$ orbitals is lifted in the presence of A-type or C-type AF states. More importantly, the A-type and C-type AF states lead to different orbital orderings: the occupation of d_{xy} orbitals is larger (smaller) than that of $d_{yz/zx}$ orbitals in the case of the C-type (A-type) AF state. Recall that the current calculations are based on the cubic structure; the observed orbital ordering must be purely due to the effect of magnetic orderings. If we evaluate the orbital polarization as the occupation number difference between the d_{xy} and the $d_{yz/zx}$ orbitals, defined as $n_p = n_{d_{xy}} - n_{d_{yz/zx}}$, the calculated values suggest that the polarization is about $n_p = -0.04$ and $n_p = 0.06$ electrons for the A-type and C-type AF states, respectively.

Now we have to answer several important questions: (i) Why are the types of orbital ordering for A-type and C-type AF states opposite? (ii) Why is the C-type AF state more stable than the A-type AF state? To answer these questions, a detailed understanding of the superexchange is important. Through the superexchange mechanism, the system gains energy from hybridizations; the hybridization between the occupied states (at one site) and the unoccupied states (at neighboring sites) will lower the energy of the occupied states by approximately t^2/Δ, where t is an effective transfer integral and Δ is the energy difference between the occupied and unoccupied states, as shown in figure 11. We start from the C-type AF state in which the spins of two adjacent Cr^{4+} ions lie antiparallely in the ab-plane but parallelly along the c-axis. The occupied majority spin d_{xy}($d_{yz/zx}$) orbital is pushed down by hybridization with the unoccupied majority spin d_{xy} ($d_{yz/zx}$) orbital located at the nearest-neighboring Cr site

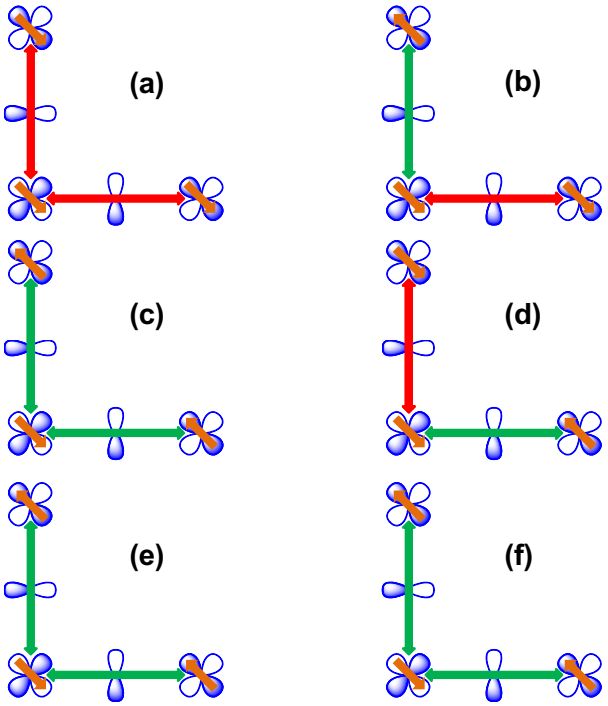

Figure 11. Cr-t_{2g} orbital hybridization through the superexchange mechanism for various AF states. The left column shows the hopping process in the **ab**-plane, the right column shows the hopping process in the **ac**- or **bc**-plane, the top row for the A-type AF state, the middle row for the C-type AF state and the bottom row for the G-type AF state; orbitals with four and two lobes are Cr-t_{2g} and O-2p orbitals, respectively; red arrows symbolize disapproval of the hopping process, green arrows symbolize approval of the hopping process and orange arrows symbolize spin ordering on Cr^{4+} ions. (a) d_{xy} orbital hybridization among adjacent Cr^{4+} ions for the A-type AF state; (b) $d_{zy/zx}$ orbital hybridization among adjacent Cr^{4+} ions for the A-type AF state; (c) d_{xy} orbital hybridization among adjacent Cr^{4+} ions for the C-type AF state; (d) $d_{zy/zx}$ orbital hybridization among adjacent Cr^{4+} ions for the C-type AF state; (e) d_{xy} orbital hybridization among adjacent Cr^{4+} ions for the G-type AF state; (f) $d_{zy/zx}$ orbital hybridization among adjacent Cr^{4+} ions for the G-type AF state.

in the ab-plane (the effect is forbidden along the c-axis due to the parallel spin chain). Such a hybridization process can occur four times for the d_{xy} orbital, but only two times for the $d_{yz/zx}$ orbital owing to its spacial orientation, as shown in figures 11(c) and (d). Therefore, the occupied majority spin d_{xy} orbital is pushed down more strongly than the $d_{yz/zx}$ orbitals, owing to the larger hybridization. Applying the same analysis to the A-type AF state in which the spins of two adjacent Cr^{4+} ions lie parallel in the ab-plane but antiparallel along the c-axis, only the hybridization paths along the c-axis need to be considered. Now, for the A-type AF state, the hybridization process can occur two times for the $d_{yz/zx}$ orbital, but zero times for the d_{xy} orbital again because of its spacial orientation, as shown in figures 11(a) and (b). Therefore, the $d_{yz/zx}$ state is lower than the d_{xy} state for the A-type AF state, the opposite of the situation in the C-type AF state. This will answer the first question listed above. For the same reason, the system

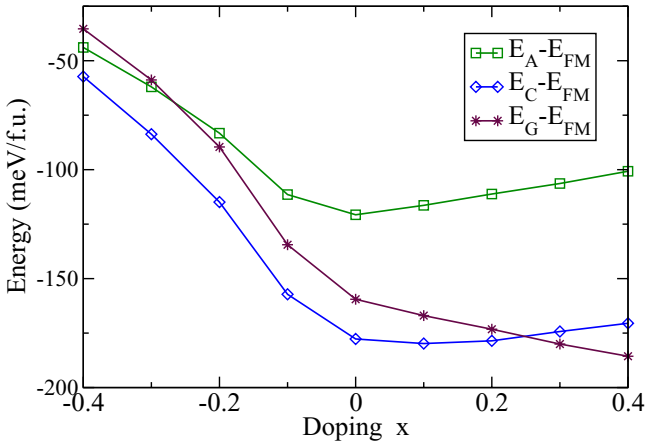

Figure 12. Calculated total energy (relative to the FM spin state) as a function of charge doping by VCA.

can gain energy from eight possible hybridization paths in the C-type AF state, but only four paths in the A-type AF state. That is why the C-type AF state is more stable than the A-type AF state.

According to the above mechanism, it is immediately realized that in the G-type AF state, three t_{2g} orbitals are evenly hybridized as shown in figures 11(e) and (f); hence no orbital ordering occurs, as shown in figure 10; there are 12 hybridization paths to relieve the total energy in the G-type AF state, so it should be more stable than the A-type or C-type AF state. Why is this not the case for first-principles calculations? The reason is as follows: applying the superexchange mechanism in the above discussion, we assume that the majority spin d_{xy} or $d_{yz/zx}$ orbitals are fully occupied. This is, of course, not the case; due to the large bandwidth and the small splitting between these t_{2g} orbitals, the system is always metallic and these t_{2g} states are partially occupied. In this situation, the Stoner mechanism, which favors itinerant ferromagnetism because of the kinetic energy gain, also plays a role and, finally, the full AF state (i.e. the G-type AF state) loses its energy gain. The system prefers to keep certain FM spin orientations along particular directions, such as the c-axis in the C-type and the ab-plane in the A-type AF state. Therefore, the stabilization of the C-type AF state comes from the subtle balance between the itinerant Stoner mechanism and the superexchange mechanism.

To further prove the above discussion, we performed the following calculations. Keeping the cubic lattice structure, we calculate the energy difference between various magnetic states as a function of the number of electrons. The VCA [20] is used here to simplify our studies. For the parent compound, the total number of t_{2g} electrons on Cr^{4+} is 2. By increasing the number of d electrons, the majority spin t_{2g} states tend to be fully occupied. As we can see from figure 12, if we increase the number of electrons, indeed the G-type AF state is stabilized.

3.3. Effect of lattice distortion

In this section, we try to elucidate the impact of tetragonal lattice distortion on the electronic structure. In the above analysis, only the cubic structure is treated. However, the tetragonally distorted structure is also observed experimentally; the possible tetragonal distortion and its effect on electronic structure must be studied. The tetragonal phase must be energetically

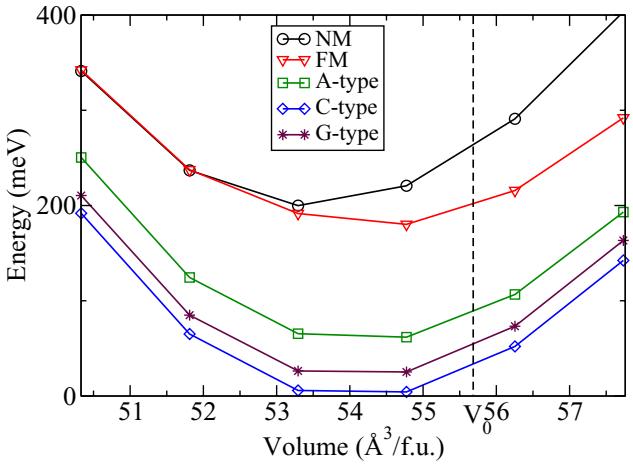

Figure 13. Calculated total energy versus volume for all kinds of spin states by LDA. The lattice distortion (c/a ratio) is optimized for each fixed volume, and V_0 is the experimental volume.

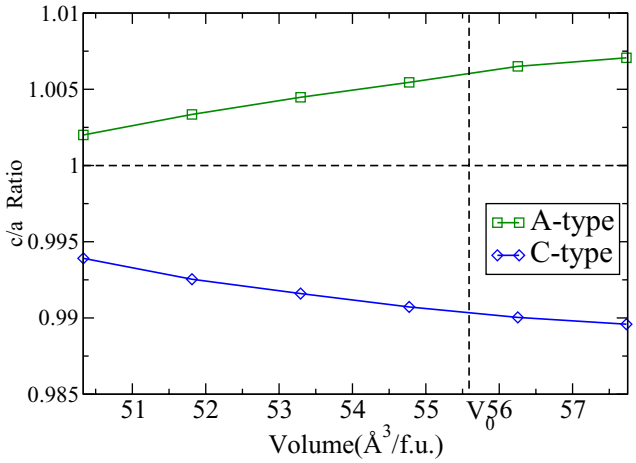

Figure 14. Optimized lattice distortion (c/a ratio) for A-type and C-type AF states at different volumes. Volume compression will suppress the lattice distortion. V_0 is the experimental volume.

very close to the cubic phase, owing to the reported coexistence of these two phases at low temperature [7].

Figure 13 shows the optimized total energy as a function of volume after allowing tetragonal distortion. Compared with the cubic results shown in figure 5, the qualitative picture is not changed at all. The C-type AF state is still the most stable state, and a big energy difference exists between the FM state and various AF states. However, what is interesting is that the C-type AF state favors compressed distortion, and the A-type AF state favors elongation distortion along the c-axis, as shown in figure 14. For the most stable C-type AF state, the optimized c/a ratio is 0.990, in good agreement with the experimentally observed tetragonal distortion ($c/a = 0.992$). Such an opposite tendency for A-type and C-type AF states can be easily understood from the orbital polarization discussed above. In the C-type AF state, the d_{xy}

orbital is more occupied than the $d_{yz/zx}$ orbitals; therefore c-axis compression is favored, owing to the reduction in electron static potential. The opposite is true for the A-type AF state. As we expected, the lattice distortion will further enhance the orbital polarization and stabilize the A-type or C-type AF state. In reality, A-type and C-type AF states are further stabilized by only 2.0 and 6.0 meV Cr^{-1}, respectively, as compared with their cubic phase. On the other hand, the FM and G-type AF states have no energy gain due to lattice distortion.

Another important issue is the origin of orbital polarization observed in both the experimental and LDA calculations. Since both lattice distortion (due to crystal field) and AF magnetic ordering due to the superexchange mechanism can lead to orbital polarization, we have to determine which one is the dominant factor. From our LDA calculations shown in table 1, it is suggested that magnetic ordering should be the dominant factor. First of all, the energy gain due to lattice distortion is small (less than 10 meV), even smaller than the energy difference between the A-type, C-type and G-type AF states (about 20–50 meV) calculated in the cubic phase. Secondly, as shown in table 1, where the calculated orbital polarizations of various magnetic states for different c/a ratios are listed, the orbital polarization coming from lattice distortion is smaller than that coming from the superexchange effect calculated in the cubic phase.

Finally, we conclude that although tetragonal distortion is favored, the distorted phase is energetically close to the cubic phase, consistent with the experimental results for the coexistence of the two phases. On the other hand, an electronic structure transition reported experimentally around 4 GPa [5] is not observed for our calculations.

The main conclusions drawn from this section are the following: (i) If tetragonal distortion is allowed, the compression (rather than elongation) along the c-axis should be favored, consistent with experimental observation. (ii) The C-type AF state and corresponding orbital ordering are further stabilized by compressed tetragonal distortion. (iii) The energy gain due to tetragonal distortion (about 10 meV Cr^{-1}) is smaller than that due to the superexchange (about 100 meV Cr^{-1}) discussed above. (iv) The orbital polarization induced by tetragonal distortion is much smaller than that induced by magnetic ordering.

3.4. Effect of on-site Coulomb correlation

One important issue in transition metal compounds is a possible strong correlation, which cannot be treated successfully by LDA-level calculations. We therefore need to check the effect of electron correlation by advanced-level theory. Given the fact that $SrCrO_3$ should be more itinerant than $CaCrO_3$ due to the larger bandwidth and the fact that most of the electron properties calculated above using LDA for $SrCrO_3$ can be compared with experiment, we expect that the effect of on-site Coulomb U will not be significant. Nevertheless, we will show, in this section by LDA + U calculations, that the $SrCrO_3$ system is indeed not a strongly correlated system. In principle, LDA + U is a cheap technique, which is suitable for the strongly correlated AF-insulating state (large U limit); however, we will show that the LDA + U results for $SrCrO_3$ are nonphysical if large U is applied.

Figure 15 shows the calculated total energy relative to the FM state as a function of U. We can clearly see that the A-type AF state is stabilized at the large U limit ($U > 4.0$ eV), which is not consistent with experiment. More surprising is that, for the C-type AF state, an orbital ordering transition is observed, as shown in figure 16. For the small U limit, the d_{xy} orbital is more populated than $d_{yz/zx}$ orbitals; however, for the large U limit, the $d_{yz/zx}$ orbitals

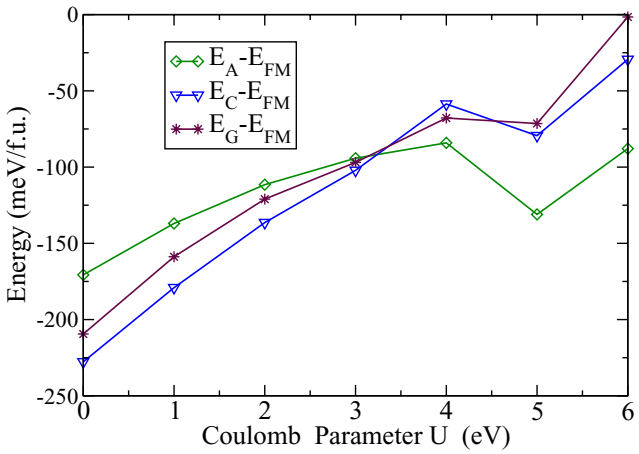

Figure 15. Calculated total energy (relative to the FM solution) of different magnetic states as a function of U by the LDA + U method.

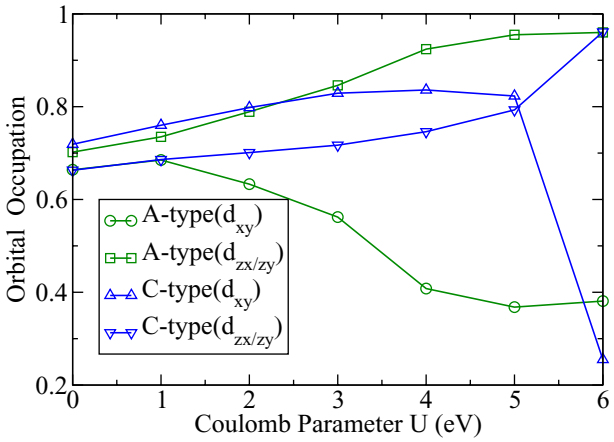

Figure 16. Orbital occupation versus correlation parameter U for A-type and C-type AF states in the cubic lattice structure calculated by LDA + U.

become more occupied, in contrast to the small U limit. The appearance of this transition can be understood as follows. In the high spin configuration of Cr^{4+}, the two 3d electrons will occupy the t_{2g} orbitals, which split into one d_{xy} orbital and two degenerate $d_{yz/zx}$ orbitals in the C-type AF state. If the d_{xy} orbital is lower in energy, the system has to be metallic due to the degeneracy between the d_{yz} and d_{zx} orbitals. However, if the U is very large (larger than bandwidth), it will try to reverse the energy level ordering of the d_{xy} and d_{yz}/d_{zx} states, in such a way that two $d_{yz/zx}$ orbitals are mostly occupied and d_{xy} becomes nearly empty; then the system gains energy from the possible gap opening between the occupied $d_{yz/zx}$ and the unoccupied d_{xy} orbitals if U is large.

The above analysis of orbital polarization suggests that, no matter whether the system is ordered in the C-type state or the A-type AF state, the $d_{yz/zx}$ orbitals are always more favored than the d_{xy} orbital in the large U limit. In such an orbital polarization, the elongated (rather than compressed) tetragonal distortion should be favored, in contrast to experimental observations. Therefore, our calculations support the conclusion that $SrCrO_3$ is not a strongly

correlated system. Furthermore, from the above studies, we also learn that the metallicity of $SrCrO_3$ in the C-type AF state is protected by the degeneracy between the d_{yz} and d_{zx} orbitals given the compressed tetragonal distortion observed. From the very good agreement between the optimized c/a ratio from LDA calculations ($c/a = 0.990$) and that observed experimentally ($c/a = 0.992$), we can further conclude that the effect of correlation is in fact very weak.

4. Summary

In summary, we study the electronic structure and magnetic property of $SrCrO_3$ systematically based on the LDA and LDA+U calculations. We analyze the various magnetic instabilities, the effect of lattice distortion and the effect of correlation. The controversial issues regarding its conductivity (metal or insulator) and lattice structure (cubic or tetragonal) can now be understood in a consistent picture. We conclude that the c-axis compressed tetragonal structure with C-type AF spin ordering is the most stable state; our calculated results are also quite consistent with available experiment results. We finally conclude that $SrCrO_3$ is a weakly correlated AF metal with a small amount of orbital polarization. Magnetic instability rather than lattice or charge instabilities plays a dominant role in this compound.

The perovskite $SrCrO_3$ compound provides a unique example of the exception to the general relation between magnetic ordering and electrical conductivity; our calculation shows clearly that metallic conductivity is due to the particular $(d_{xy})^1(d_{zx}d_{zy})^1$ orbital ordering. With a few examples of the FM insulator CrO_2 [23] that were also caused by a particular type of orbital ordering, we can infer that in transition metal compounds not only spin ordering but also orbital ordering has an impact on conductivity. We believe that there will be more and more such kinds of examples yet to be discovered; this will open up a new direction in the study of the complex interplay of spin–orbital ordering in transition metal compounds.

As we showed in the calculations above, there is C-type AF state-to-G-type AF state transition due to electron doping; this transition will be accompanied by a lattice or orbital ordering transition. To further validate the calculation, an experimental work is in progress that we will discuss in detail in future.

Acknowledgments

We acknowledge valuable discussions with H J Zhang and X Y Deng and support from the NSF of China the 973 Program of China, and the International Science and Technology Cooperation Program of China.

References

[1] Imada M, Fujimori A and Tokura Y 1998 *Rev. Mod. Phys.* **70** 1039
[2] Tokura Y and Nagaosa N 2000 *Science* **288** 462
[3] Dagotto E 2005 *Science* **309** 257
[4] Fang Z, Terakura K, Sawada H, Miyazaki T and Solovyev I 1998 *Phys. Rev. Lett.* **81** 1027
[5] Zhou J-S, Jin C-Q, Long Y-W, Yang L-X and Goodenough J B 2006 *Phy. Rev. Lett.* **96** 046408
[6] Chamberland B L 1967 *Solid State Commun.* **5** 663
[7] SanMartin L O, Williams A J, Rodgers J, Attfield J P, Heymann G and Huppertz H 2007 *Phy. Rev. Lett.* **99** 255701

[8] Arevalo-Lopez A M, Castillo-Martinez E and Alario-Franco M A 2008 *J. Phys: Condens. Matter* **20** 505207
[9] Alario-Franco M A, Castillo-Martinez E and Arevalo-Lopez A M 2009 *High Press Res.* **29** 254
[10] Lee K-W and Pickett W E 2009 *Phy. Rev.* B **80** 125133
[11] Streltsov S V, Korotin M A, Anisimov V I and Khomskii D I 2008 *Phy. Rev.* B **78** 054425
[12] Komarek A C *et al* 2008 *Phys. Rev. Lett.* **101** 167204
[13] Argyriou D N, Mitchell J F, Radaelli P G, Bordallo H N, Cox D E, Medarde M and Jorgensen J D 1999 *Phys. Rev.* B **59** 8695
[14] Yoshida Y, Ikeda S-I, Matsuhata H, Shirakawa N, Lee C H and Katano S 2005 *Phys. Rev.* B **72** 054412
[15] Goodenough J B 1963 *Magnetism and the Chemical Bond* (New York: Interscience)
[16] Fang Z and Terakura K 2002 *J. Phys.: Condens. Matter* **14** 3001
[17] Payne M C, Teter M P, Allan D C, Arias T A and Joannopoulos J D 1992 *Rev. Mod. Phys.* **64** 1045
[18] Laasonen K, Car R, Lee C and Vanderbilt D 1991 *Phys. Rev.* B **43** 6796
[19] Rappe A M, Rabe K M, Kaxiras E and Joannopoulos J D 1990 *Phys. Rev.* B **41** 1227
[20] Bellaiche L and Vanderbilt D 2000 *Phys. Rev.* B **61** 127877
[21] Fang Z and Nagaosa N 2004 *Phys. Rev. Lett.* **93** 176404
[22] Fang Z, Nagaosa N and Terakura K 2003 *Phys. Rev.* B **67** 035101
[23] Brener N E, Tyler J M, Callaway J, Bagayoko D and Zhao G L 2000 *Phys. Rev.* B **61** 16582
Khomskii D I and Sawatzky G 1997 *Solid State Commun.* **102** 87